ANALYSIS OF THE MICROSTRUCTURE AND ENERGY ABSORPTION CAPACITY OF HIGH-MANGANESE TWIP STEEL DEFORMED UNDER STATIC AND DYNAMIC LOADING CONDITIONS

[1]Michał KOSTKA, [2]Katarzyna JASIAK, [1]Mikołaj KONOFOL, [1]Mateusz WESOŁOWSKI, [1]Iwona BEDNARCZYK, [1]Marek TKOCZ, [2]Zbigniew GRONOSTAJSKI, [1]Magdalena B. JABŁOŃSKA

[1]Silesian University of Technology, Gliwice, Poland, EU, michal.kostka@polsl.pl

[2]Wrocław University of Science and Technology, Wrocław, Poland, EU

https://doi.org/10.37904/metal.2024.4884

Abstract

The work concerns the analysis of the effect of deformation under static and dynamic conditions of high-manganese X42 steel with the SFE value of 24 mJ/m^2 on energy absorption capacity and microstructure. X42 steel is graded as a steel that strengthens by mechanical twinning (TWIP effect). TWIP steels have an excellent combination of strength and ductility properties, making them an excellent material for use in controlled crumple zone components for vehicles. A static tensile test and a flywheel machine tensile test at a strain rate corresponding to dynamic conditions were carried out for the tested steel. Microstructure studies were carried out using light microscopy and scanning electron microscopy techniques. From the stress-strain curves, the value of the energy absorbed during plastic deformation was calculated. On the base of the tensile tests, it can be concluded that the material strengthens with the increase in strain rate without losing its good plastic properties. Analysis of the microstructure showed deformation effects in the form of austenite grains elongated in the direction of the tensile direction, within which mechanical twins and deformation bands are formed and the intensity of the generation of twins is correlated to the strain rate. The value of absorbed energy during plastic deformation of the tested steel is at a similar level compared to other TWIP steels expected to be used for structural components absorbing energy during impact.

Keywords: TWIP steel, deformation, energy absorption, strain rate, twinning

1. INTRODUCTION

Currently, the most promising group of steels under development for automotive applications are those belonging to the so-called Advanced High Strength Steel (AHSS) group [1]. This group includes, among others, high-manganese steels [2]. Among these, twinning-induced plasticity (TWIP) steels are particularly interesting for use in vehicle safety zone sections [3]. They achieve the highest values of absorbed strain energy E_{ABS} and are therefore envisaged for use as energy absorbing elements in the crumple zones of vehicles [4]. The main deformation mechanism in TWIP steels, under both static and dynamic deformation conditions, is twinning [5]. In addition to the strain rate, the twinning mechanism is also influenced by the value of the strain [6]. Mechanical twinning occurs in high-manganese steels with a stacking fault energy (SFE) in the range of 20-60 mJ/m^2 [3]. As indicated by Curtze and Kuokkala [7], research on TWIP steels is conducted under both static and dynamic deformation conditions. Tests under static conditions help to understand the mechanisms responsible for the strengthening of the material, while those conducted under dynamic conditions reflect the conditions arising during road traffic collisions. TWIP steels exhibit an increase in strength properties with an increased strain rate, without affecting their total elongation, which remains at a similar level [8]. A literature analysis of TWIP steels indicates that deformation under static conditions triggers, in addition to the classical dislocation slip, a twinning mechanism as favoured in manganese steels [9]. Initially, only one twinning system

is activated, but with increasing deformation values, additional systems are activated. When shifting into the dynamic strain rate, secondary systems of twinning may be triggered [10].

2. RESEARCH MATERIAL AND METHODOLOGY

The test material was high-manganese steel X42 with the chemical composition shown in Table 1. The material is characterised by a single-phase austenitic structure with visible annealing twins. The steel was designed at Faculty of Materials Engineering of Silesian University of Science and Technology and manufactured according by [11]. In order for X42 steel to be classed as a TWIP steel, it had to have an SFE value of 20-60 mJ/m^2. In an attempt to verify the SFE, calculations were performed, using the amount of Fe, Mn, Al, and C, according to the formulas proposed by Zambrano [12]. The calculated value of SFE for X42 steel is 24 mJ/m^2.

Table 1 Chemical composition of high-manganese steel X42

Steel grade	Chemical composition, % wt									
	C	Mn	Al	B	P	S	Ce	La	Nd	Fe
X42	0.42	21	2.6	0.0020	<0.01	0.006	0.011	<0.005	<0.005	balance

Static tensile tests were carried out using an Instron 3369 machine at the Department of Metal Forming, Welding and Metrology, Faculty of Mechanics, Wrocław University of Science and Technology. The tests were performed on X42 high-manganese steel specimens at a strain rate of: 0.001 s^{-1}, the test was carried out on two specimens (specimen 1 & 2). During the tensile process, the elongation of the specimens was measured using an extensometer with a measuring length of 50 mm. Using strain-stress characteristics the yield strength $R_{p0.2}$, the tensile strength R_m, and the strain ε, were determined.

Dynamic tensile tests at a strain rate of 1000 s^{-1} were conducted using a flywheel machine. Two specimens (specimen 3 and 4) with a gauge length of 14 mm were used. Strains were determined using the Digital Image Correlation (DIC) technique, which involves applying a grid of points to the measured specimen and then tracking and analysing the displacement of these points relative to each other in successive images taken during the deformation of the specimen.

Materials used for energy-absorbing components, which include TWIP steels, must have a high absorbed energy value [4]. This can be determined using equation (1) [4].

$$E_{ABS} = \frac{W_U}{V} \quad (1)$$

where:

W_U – work of deformation at break (J),

V – volume of the measurement base (mm^3).

The work of strain at break was determined as the area under the flow function on the consolidation diagram Excel was used to calculate the plastic deformation work. The dependence of actual strain on strength is shown at figure 1. To calculate the strain work (orange area in Figure 1), equation (2) was used. With the work value, the absorbed energy was calculated according to equation (1).

$$W_U = V \cdot \int_0^{\varphi} \sigma_P(\varphi) \cdot d\varphi \quad (2)$$

where:

σ_p – flow stress (MPa),

φ – true strain (-).

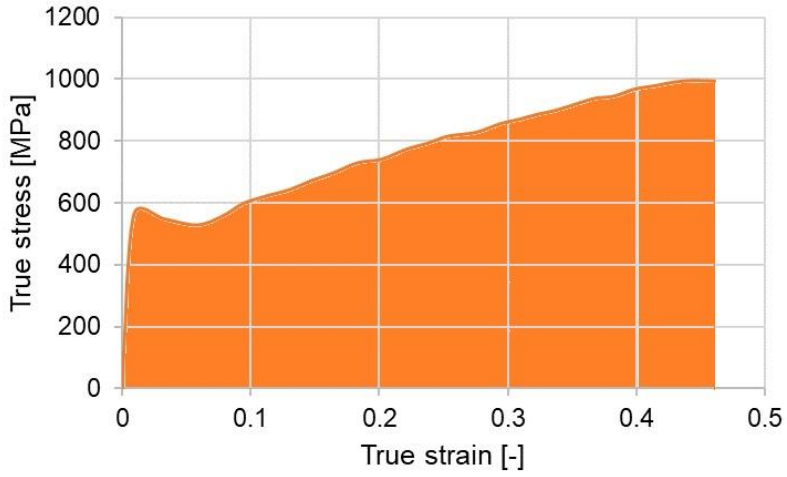

Figure 1 Plot of true strain vs. stress with the area under the curve marked - as the value of strain work

Observations of the microstructure of the test steel after the tensile test were carried out on a test piece parallel to the specimen axis (longitudinal). For specimens in tension under static conditions, observations were carried out sequentially starting from the point of specimen rupture in depth (approximately 5 mm from the point of fracture), over the entire surface, while for specimens in dynamic tension the observation was carried out at the point of rupture and in the region of 30 - 50% deformation.

Metallographic investigations were carried out using an Olympus GX71 light microscope. The examinations included observations of the specimens after the tensile tests. Magnification of 50x, 100x and 200x was used. To reveal the microstructure, the material was etched in reagent: Nital 6% - (94 ml ethanol, 6 ml HNO_3 acid). Microstructure studies using scanning electron microscopy (SEM) techniques were performed with a Hitachi S-3400N microscope.

3. RESEARCH RESULTS

The results of the static tensile test are shown in Figure 2a. The yield strength of X42 steel deformed at 0.001 s^{-1} is 233 MPa for deforming specimen 1 and 236 MPa when deforming specimen 2. The steel reaches a tensile strength of 574 MPa during deformation of specimen 1 and 581 MPa for specimen 2. The steel has very good ductility properties, with elongation reaching 71% for both samples. The results after the tensile test under dynamic conditions are shown in Figure 2b. The yield strength of X42 steel deformed at 1000 s^{-1} is 485 MPa for the deformation of specimen 3 and 487 MPa when specimen 4 is deformed. The steel reaches a tensile strength of 662 MPa when specimen 3 is deformed and 650 MPa for specimen 4. The steel has good ductility properties, with total elongation reaching 65% for specimen 3 and 59% for specimen 4. The resulting values for the conventional yield strength $R_{p0.2}$, tensile strength R_m and strain ε are shown in Table 2. The results obtained are similar to the other TWIP steels tested by, among others: Curtze & Kuokkala [7], Dobrzański et al. [5] and Gronostajski et al. [13]

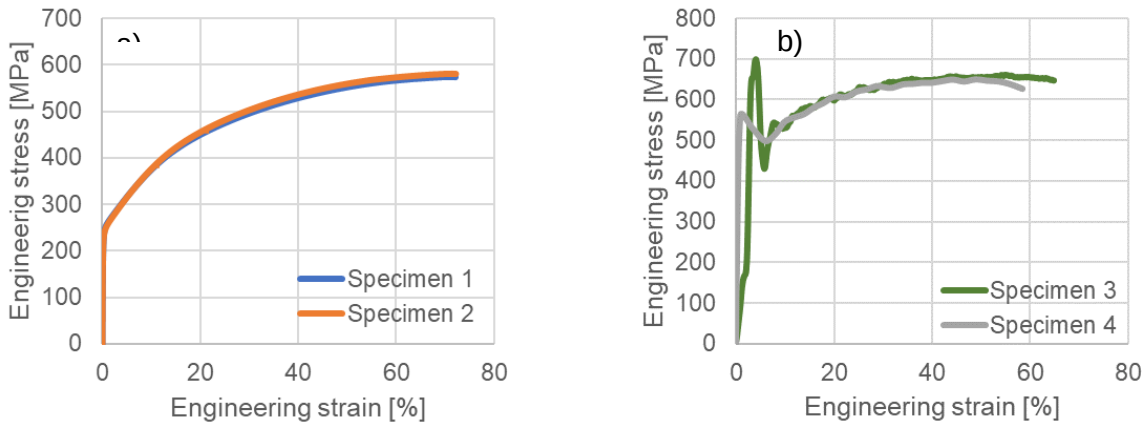

Figure 2 Stress curves for tensile tests under a) static and b) dynamic conditions

Table 2 Tensile strength, yield strength and total elongation obtained from tensile tests for X42 steel

Strain rate	**R_m**	**$R_{p0,2}$**	**ε_{max}**
[s^{-1}]	[MPa]	[MPa]	[%]
0.001	581	263	71
1000	662	487	65

Calculations of plastic strain work and absorbed energy were made from tensile curves of selected specimens, for strain values of: 0.2, 0.3 and 0.45. The results of calculations for X42 steel deformed at 0.001 s^{-1} and 1000 s^{-1} are summarised in Tables 3 and 4.

Table 3 Results of calculating plastic strain work for static and dynamic strain rates for different strain values

Strain rate s^{-1}	**Plastic strain work W_U, J**		
	ε = 0,2	ε = 0,3	ε = 0,45
0.001	114	200	354
1000	184	300	476

Table 4 Results of the calculation of absorbed energy for static and dynamic strain rates for different strain values

Strain rate s^{-1}	**Absorbed energy E_{ABS}, J/mm^3**		
	ε = 0.2	ε = 0.3	ε = 0.45
0.001	0.08	0.15	0.26
1000	0.14	0.21	0.35

Analysing the results obtained for both absorbed energy and deformation work, it can be seen that, for each strain value, the values of the given properties are higher for specimens deformed at dynamic strain rates.

The microstructure of the tested steel after the static tensile test revealed deformation effects in the form of austenite grains elongated in the force direction, within which mechanical twinning and shear bands occur (Figure 3a, c). Closer to the fracture the grains are more elongated, and the twinning effect is more intensive. In this zone, twins are generated in two twinning systems, while only one twinning system is present

at a location distant from the fracture. A similar change in structure was observed by Feng et al. [14] and Gutierrez-Urruita & Raabe [6]. The microstructure after the dynamic tensile test (Figure 3b, d) is very similar in the zone close to the fracture and the one away from it. The intensity of the generation of twins is very high, the austenite grains have been deformed, twins are generated in three systems of twinning.

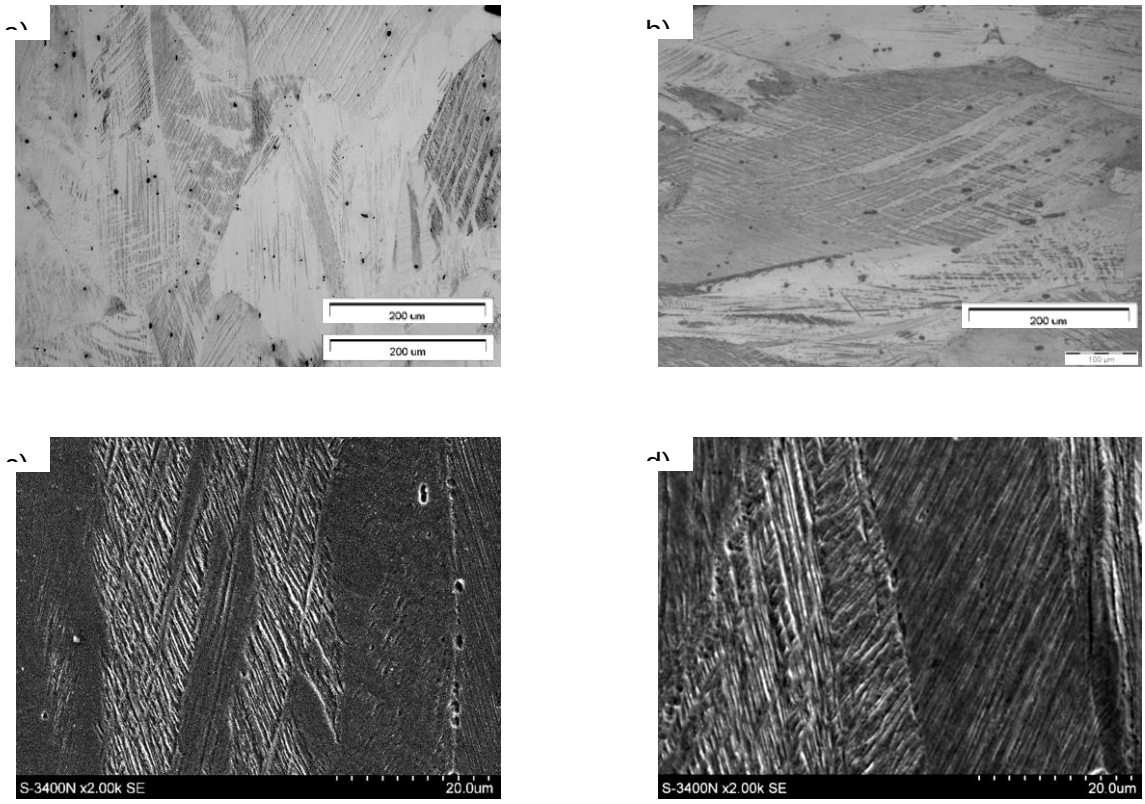

Figure 3 Microstructure of X42 steel a), b) light microscopy; c), d) SEM

4. CONCLUSION

The study is an analysis of the mechanical properties and microstructure of the high-manganese steel X42, which belong to the group of steels strengthened by mechanical twinning (TWIP effect), subjected to deformation in a standard tensile test on a testing machine, i.e. under static conditions, and to so-called dynamic deformation using a flywheel machine. Analyzing the results obtained for the mechanical properties of the steel tested, based on tensile tests under static (0.001 s^{-1}) and dynamic (1000 s^{-1}) conditions, it can be concluded that the material strengthens with an increase in strain rate. The tensile strength in dynamic stretching was 70 MPa above that of static conditions and the yield strength more than doubled for a specimen deformed at 1000 s^{-1}. At the same time, despite the increase in strain rate, the plastic properties remain at a similar level. The microstructure tests carried out showed that, irrespective of the strain rate, the steel studied shows a strong tendency to twinning. The X42 steel tested has an absorbed energy value during deformation of 0.35 J/mm^3. The determined value of the E_{ABS} index is at a good level in comparison with other steels tested by Madivala & Bleck (0.43 J/mm^3) [4] and Wesselmecking et al. (0.37 J/mm^3) [15], used for energy absorbing structural components in controlled crush zones of vehicles.

ACKNOWLEDGEMENTS

Work carried out within the framework of the project [grant number UMO-2019/35/B/ST8/02184] " Effect of the heat generated during deformation at high strain rates on the structure and properties of high manganese steels with twinning as the dominant deformation mechanism" financed by The NCN.

REFERENCES

[1] GRAJCAR A., KUZIAK R., and ZALECKI W. “Third generation of AHSS with increased fraction of retained austenite for the automotive industry”. *Archives of Civil and Mechanical Engineering*. 2012, vol. 12, no. 3, pp. 334–341. doi: 10.1016/j.acme.2012.06.011.

[2] FOJT-DYMARA G., OPIELA M., and BOREK W. “Susceptibility of High-Manganese Steel to High-Temperature Cracking”. *Materials*. 2022. vol. 15, no. 22, pp. 8198. doi: 10.3390/ma15228198.

[3] JABŁOŃSKA M.B., ŚMIGLEWICZ A., and NIEWIELSKI G. “The effect of strain rate on the mechanical properties and microstructure of the high-Mn steel after dynamic deformation tests”. *Archives of Metallurgy and Materials*. 2015, vol. 60, no. 2A, pp. 577–580. doi: 10.1515/amm-2015-0176.

[4] MADIVALA M. and BLECK W. “Strain Rate Dependent Mechanical Properties of TWIP Steel,” *JOM*. 2019. vol. 71, no. 4, pp. 1291–1302. doi: 10.1007/s11837-018-3137-0.

[5] DOBRZAŃSKI L.A., BOREK W., and MAZURKIEWICZ J. “Influence of high strain rates on the structure and mechanical properties of high-manganes austenitic TWIP-type steel”. *Materialwissenschaft und Werkstofftechnik*. 2016. Wiley-VCH Verlag, pp. 428–435. doi: 10.1002/mawe.201600518.

[6] GUTIERREZ-URRUTIA I. and RAABE D. “Dislocation and twin substructure evolution during strain hardening of an Fe-22 wt.% Mn-0.6 wt.% C TWIP steel observed by electron channeling contrast imaging”. *Acta Mater*. 2011, vol. 59, no. 16, pp. 6449–6462, doi: 10.1016/j.actamat.2011.07.009.

[7] CURTZE S. and KUOKKALA V.T. “Dependence of tensile deformation behavior of TWIP steels on stacking fault energy, temperature and strain rate”. *Acta Mater*. 2010 vol. 58, no. 15, pp. 5129–5141. doi: 10.1016/j.actamat.2010.05.049.

[8] BENZING J.T., *et al.* “Effects of strain rate on mechanical properties and deformation behavior of an austenitic Fe-25Mn-3Al-3Si TWIP-TRIP steel”. *Materials Science and Engineering: A*. 2018, vol. 711, pp. 78–92, doi: 10.1016/j.msea.2017.11.017.

[9] SAEED-AKBARI A., IMLAU J., PRAHL U. and BLECK W. “Derivation and variation in composition-dependent stacking fault energy maps based on subregular solution model in high-manganese steels”. *Metall Mater Trans A Phys Metall Mater Sci*. 2009, vol. 40, no. 13, pp. 3076–3090. doi: 10.1007/s11661-009-0050-8.

[10] SAHU P., CURTZE S., DAS A., MAHATO B., KUOKKALA V.T., and CHOWDHURY S.G. “Stability of austenite and quasi-adiabatic heating during high-strain-rate deformation of twinning-induced plasticity steels”. *Scr Mater*. 2010, vol. 62, no. 1, pp. 5–8. doi: 10.1016/j.scriptamat.2009.09.010.

[11] JASIAK K., GRONOSTAJSKI Z., and JABŁOŃSKA M.B. “Experimental and numerical determination of the temperature of TWIP steel during dynamic tensile testing”. *Journal of Materials Research and Technology*. 2024. vol. 28, pp. 856–864. doi: 10.1016/j.jmrt.2023.12.056.

[12] ZAMBRANO O.A. “Stacking fault energy maps of Fe-Mn-Al-C-Si steels: Effect of temperature, grain size, and variations in compositions,” *Journal of Engineering Materials and Technology, Transactions of the ASME*. 2016. vol. 138, no. 4, pp. 041010. doi: 10.1115/1.4033632.

[13] GRONOSTAJSKI Z., NIECHAJOWICZ A., KUZIAK R., KRAWCZYK J., and POLAK S. “The effect of the strain rate on the stress- strain curve and microstructure of AHSS”. *J Mater Process Technol*. 2017, vol. 242, pp. 246–259. doi: 10.1016/j.jmatprotec.2016.11.023.

[14] FENG X., LIU X., BAI S., YE Y., ZONG L. and TANG Y. “Mechanical properties and deformation behaviour of TWIP steel at different strain rates”. *Materials Science and Engineering: A*. 2023, vol. 879, pp. 145182. doi: 10.1016/j.msea.2023.145182.

[15] WESSELMECKING S., KREINS M., DAHMEN M., and BLECK W. “Material oriented crash-box design – Combining structural and material design todoc_improve specific energy absorption,” *Mater Des*. 2022. vol. 213, pp. 110357. doi: 10.1016/j.matdes.2021.110357.